Wireless Networks (2020) 26:1519–1534
https://doi.org/10.1007/s11276-019-02210-4

Enhanced scheduling schemes with energy conservation for dynamic point selection in cloud radio access networks

Ching-Kuo Hsu[1] · Jia-Ming Liang[2,3] · Kun-Ru Wu[1] · Jen-Jee Chen[4] · Yu-Chee Tseng[1]

Published online: 17 December 2019

Abstract

In 5G mobile communications, *Cloud-RAN* (*C-RAN*) (Camps-Mur et al. in IEEE Commun Mag 57:99–105, 2019) is proposed to provide broadband services. It separates computation entities, i.e., *baseband units* (*BBUs*), from *base stations* and puts all BBUs in a centralized cloud. Existing researches have investigated how to enhance *user equipments* (*UEs*) to receive data from multiple collaborative cells by leveraging the *dynamic point selection (DPS)* technology. Collaborative transmission may cause higher energy consumption for UEs. Although 3GPP has defined the *discontinuous reception* (*DRX*) mechanism by regulating UEs to turn off their radio interfaces in a periodical manner, how to well coordinate DRX with DPS under the C-RAN architecture is still left as an open issue. This paper is the first one addressing this resource optimization problem in C-RAN with DPS, which asks how to optimize DRX parameters of UEs by considering their *quality-of-service* (*QoS*). We prove this problem to be NP-complete, and then propose two effective and efficient DPS solutions, called *serving-ratio (SR)* scheme and *cost-aware* (*CA*) scheme. SR serves UEs based on a special 'serving ratio' to ensure UEs receiving continuous subframes, especially for those in cell intersections. On the other hand, CA exploits the strategies of minimal scheduling costs to balance energy and throughput efficiency in a perspective way. Extensive simulation results validate that our schemes can successfully achieve higher system throughput, provide better resource utilization, and serve more UEs while guaranteeing their QoS and saving considerable energy as compared to existing schemes.

Keywords 5G · Cloud radio access network (C-RAN) · Discontinuous reception (DRX) · Dynamic point selection (DPS) · Power saving · Sleep scheduling

✉ Jia-Ming Liang
jmliang@mail.cgu.edu.tw

Ching-Kuo Hsu
HSUck@cs.nctu.edu.tw

Kun-Ru Wu
kunruwu@cs.nctu.edu.tw

Jen-Jee Chen
jenjee@nctu.edu.tw

Yu-Chee Tseng
yctseng@cs.nctu.edu.tw

[1] Department of Computer Science, National Chiao Tung University, Hsinchu 30010, Taiwan

[2] Department of Computer Science and Information Engineering, Chang Gung University, Taoyuan 33302, Taiwan

[3] Department of General Medicine, Chang Gung Memorial Hospital, Taoyuan 33378, Taiwan

[4] College of Artificial Intelligence and Green Energy, National Chiao Tung University, Hsinchu 30010, Taiwan

1 Introduction

Cloud Radio Access Network (C-RAN) has received a lot of attention recently [1–3]. It has a centralized network architecture that separates baseband units (BBUs) from base stations (BSs), puts BBUs in a cloud pool, and leaves remote radio heads (RRHs) at cell sites. Thus, it can collaborate cells centrally to enhance system throughput [4–7], reduce inter- and intra-cell interference to increase spectrum utilization and system capacity [8–10], and further ensure the traffic delay and satisfy the requirements of UEs [11–13]. One of the C-RAN technology is *dynamic point selection (DPS)* [14], which allows a UE to be collaboratively served by multiple RRHs. Collaborative transmission may cause higher energy consumption for UEs. Although 3GPP (the 3rd Generation Partnership Project) [15] has defined the *discontinuous reception (DRX)* mechanism by allowing a UE to turn off its radio interface when its evolved Node B (eNB) has no data for it, how to optimize the DRX parameters to minimize the energy consumption of UEs under the C-RAN with DPS architecture is still an open issue.

In this paper, we address the DRX optimization problem under given QoS constraints of UEs in C-RAN with DPS. The objective is to minimize the wake-up periods of UEs while satisfying their QoS requirements in terms of data rate and packet delay. We model it as an optimization problem and prove it to be NP-complete. We then propose two heuristic scheduling schemes, called *serving-ratio* (SR) scheme and *cost-aware* (CA) scheme. The goal of SR is to avoid UEs' unnecessary wake-up periods by serving the UEs with smaller remaining serving ratio first. On the other hand, CA exploits front cost and internal cost metrics to avoid the allocated resource separately and further improve resource utilization while maintaining energy efficiency.

The main contributions of this paper are three-fold. First, this is the first complete work addressing the energy conservation issue under the C-RAN architecture by optimizing both DRX parameters and DPS scheduling.[1] Second, we prove this problem to be NP-complete by reducing it to the multi-dimensional knapsack problem [17]. We then point out three key factors to improve system throughput and energy consumption: (a) effective pairing of cells and UEs, (b) serving UEs with the minimal scheduling cost to better utilize resource, and (c) allocating resource to edge UEs continuously to avoid unnecessary wake-up periods. Based on these perspectives, we propose SR and CA schemes, which incur time complexities of $O(NlogN)$ and $O(N^2)$, respectively. Third, we show that SR can well decrease UEs' energy consumption and CA can further enhance system throughput and resource utilization. Our simulation results validate that jointly solving DPS and DRX can increase 17–25% of system throughput in average and save at least 50% of UEs' energy, compared to existing schemes.

The rest of this paper is organized as follows. Related work is discussed in Sect. 2. Preliminaries are given in Sect. 3. Section 4 presents our schemes. Simulation results are shown in Sect. 5. Conclusions are drawn in Sect. 6.

2 Related work

Resource optimization has been intensively studied for C-RAN. References [3–13] consider traffic scheduling under C-RAN with DPS. Reference [3] analyzes the performance of DPS networks. The study [4] proposes a load- and channel-aware DPS algorithm to enhance system throughput. The study [5] presents a message-passing-based DPS scheme for coordinated transmission to increase sum rate. The work [6] proposes a joint cell assignment scheme for downlink throughput maximization. The work [7] proposes a benefit-based multi-cell selection scheme to improve throughput of UEs. The study [8] proposes an electromagnetic-field strategy for cell selection to enhance network utilization. The work [9] develops an r-fraction cell-selection scheme to improve network capacity. The work [10] develops a dynamic hybrid clustering scheme for LTE-A networks with DPS to enhance eNB backhaul capacity. The study [11] designs two cell-loading DPS schemes to enhance cell-edge performance. The work [12] develops a cross-layer analytic model for UEs in sleeping cells to reduce traffic delay and packet loss. The study [13] proposes a dynamic resource allocation scheme to improve QoS of UEs. However, the above works do not consider the energy issue.

Energy saving under C-RAN is studied in [18–25]. The work [18] proposes a network optimization scheme to enhance energy efficiency in suburban and rural areas. The study [19] proposes a coalitional-game-theory scheme to identify the potential room for cooperation among different mobile network operators to share energy under C-RAN. The work [20] focuses on TDD C-RAN and proposes a coexisting downlink-and-uplink beamforming scheme. The work [21] considers C-RAN with dense APs and designs a joint UE-AP association and beamforming scheme. The work [22] proposes a cross-layer resource allocation scheme under C-RAN to reduce system energy consumption. The study [23] presents a cell association scheme to enhance downlink energy efficiency. The work [24] develops a traffic-aware RRH selection scheme to reduce energy consumption of C-RAN. The work [25] proposes a traffic-scattering scheme for group paging to reduce energy

[1] A preliminary version of this paper appeared in [16].

consumption of UEs. However, the above studies focus more on the lower-layer energy issue. DRX, which allows a UE to schedule its radio on-off patterns, is not well addressed for C-RAN. This motivates us to address the joint resource allocation and sleep scheduling problem in C-RAN.

3 Preliminaries

In this section, we first introduce the C-RAN architecture, followed by the DRX mechanism and the formal definition of our DRX optimization problem in DPS C-RAN.

3.1 C-RAN and DPS

C-RAN is designed to support collaborative transmissions among RRHs. As shown in Fig. 1(a), it separates a traditional base station into two parts: digital function unit BBU and radio function unit RRH. BBUs are placed in a BBU pool in a cloud and connect with RRHs via optical fibers; thus, it centralizes control. In C-RAN, DPS is a way to realize collaborative transmission. When a UE is on the borders of multiple cells, DPS can allocate multiple RRHs to serve it. An example is shown in Fig. 1(b), where two cells, $Cell_1$ and $Cell_2$, serve UE_1 simultaneously. In this example, UE_1 receives data from $Cell_1$ at time slots 1–2, and switches to $Cell_2$ at time slots 3–5. Hence, it can enhance UEs' data rates and balance RRHs' traffic loads.

3.2 DRX

To save energy of UEs, the DRX mechanism is designed to schedule downlink transmissions. The DRX configurations are UE-specific and determined by eNB. When DRX is activated, a UE performs wake-up/sleep operations in a periodic cycle. An example is shown in Fig. 2, where the basic duration is a subframe (with a length of 1 ms). There are short and long cycles; since downlink communications are usually used in real-time services, this paper focuses on the short cycle. When DRX is enabled, four parameters are defined: (1) DRX-cycle-length, (2) DRX-start-offset, (3) On-duration, and (4) InactivityTimer. The DRX-cycle-length is the period of the UE to receive data from the eNB. The DRX-start-offset is the starting subframe of DRX-cycle-length. The On-duration is the time when the UE has to stay awake to monitor any data delivered from the eNB. If any data is received, the UE starts InactivityTimer and stays awake before the timer expires. If any data is received, it resets the timer. When InactivityTimer expires, the UE goes to sleep and turns off its radio interface. During a sleep period, any data for the UE will be buffered at the eNB until the next On-duration arrives.

3.3 DRX and DPS

In this paper, we investigate how to apply DRX to DPS in C-RAN. We give an example in Fig. 3(a), where there are 3 cells ($Cell_1 \sim Cell_3$) serving 6 UEs ($UE_1 \sim UE_6$), where $Cell_1$ covers $\{UE_1, UE_3\}$, $Cell_2$ covers $\{UE_1, UE_2, UE_5, UE_6\}$, and $Cell_3$ covers $\{UE_2, UE_4\}$. Suppose that UE_1

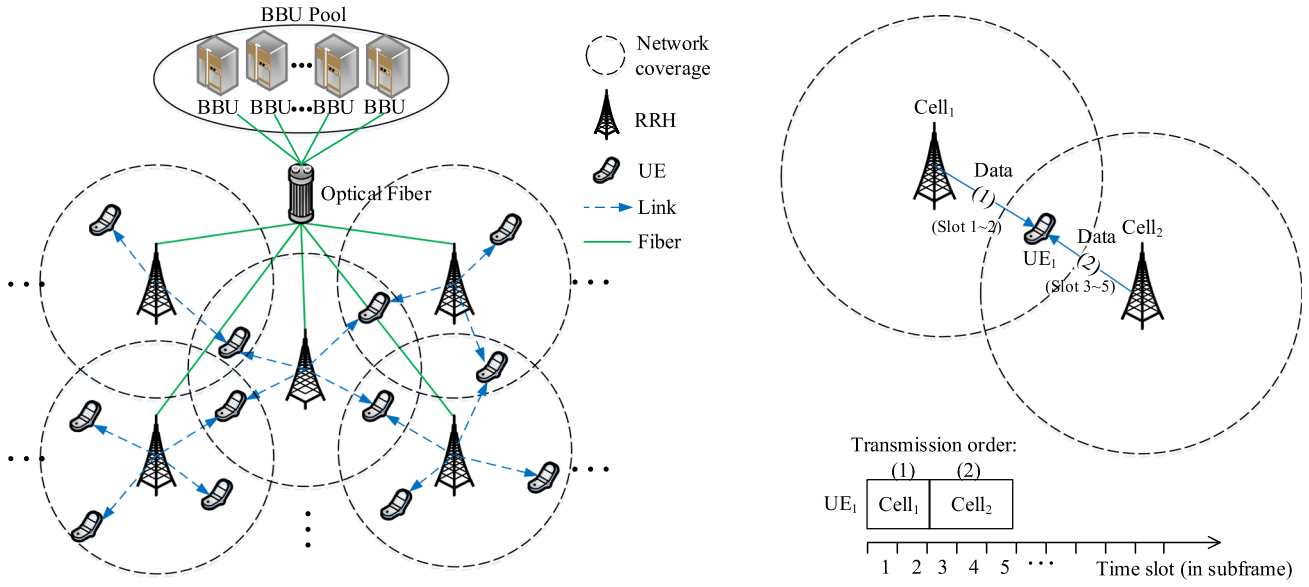

(a) network architecture of C-RAN. **(b)** Example of dynamic point selection (DPS).

Fig. 1 C-RAN architecture and an example of DPS

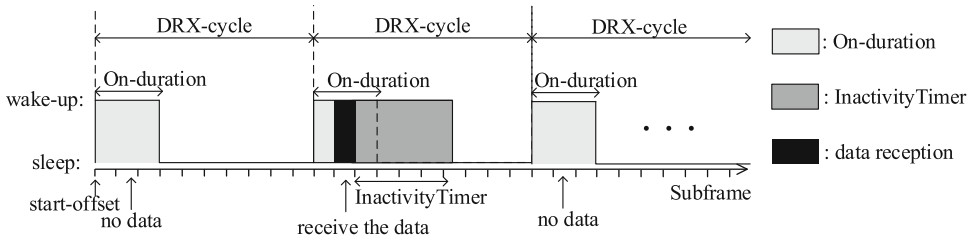

Fig. 2 An example of DRX operation

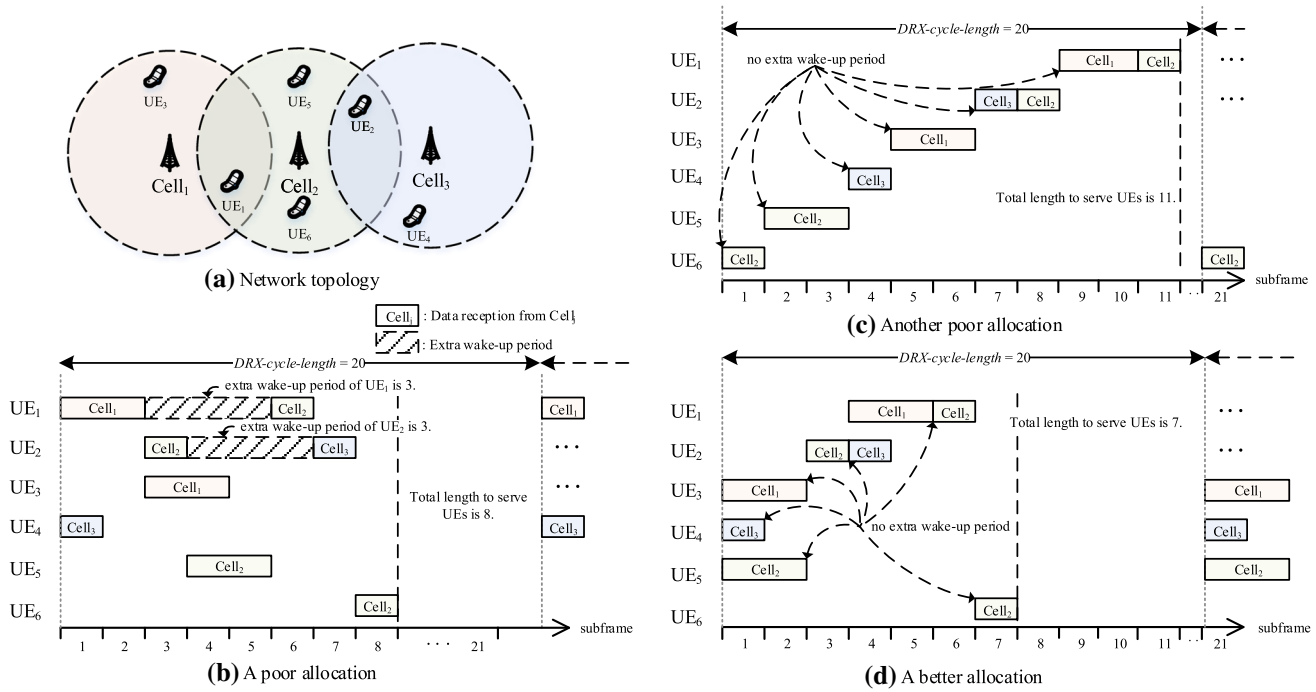

Fig. 3 Some allocation examples of DRX with DPS

needs to receive two data subframes from $Cell_1$ and one data subframe from $Cell_2$; UE_2 needs to receive one subframe from both $Cell_2$ and $Cell_3$; UE_3 needs to receive two subframes from $Cell_1$; UE_4 needs to receive one subframe from $Cell_3$; UE_5 needs to receive two subframes from $Cell_2$; UE_6 needs to receive one subframe from $Cell_2$. Let DRX-cycle-length of all UEs be 20 subframes. We illustrate the effect of different allocations in the following. Figure 3(b) shows a poor allocation, which needs 8 subframes to serve all UEs and takes 6 extra subframes per cycle for UEs to stay awake; Fig. 3(c) shows another poor allocation, which needs 11 subframes per cycle to serve all UEs, but no extra wake-up period is incurred. Figure 3(d) shows a better allocation, which takes 7 subframes per cycle to serve all UEs without any extra wake-up period. Note that even if we have reserved a wake-up period for a UE, its *actual* data reception time may vary (shorter or longer) due to channel rate variation. Our design will consider this factor.

3.4 Problem definition

We consider downlink transmission under the C-RAN architecture. There are M RRHs (or cells) to serve N UEs with DPS capability. Each UE_i, $i = 1, \ldots, N$, is served by one or more cells, denoted by serving cell set $Cell_i^{set}$, and has an admitted data rate of $R_{i,j} \geq 0$ (bits/ms) and a delay constraint of $D_{i,j}$ (ms) granted by $Cell_j \in Cell_i^{set}$. Note that $R_{i,j}$ can be zero if UE_i is not granted any data from $Cell_j$. The subframe duration is 1 ms and the basic allocation unit in a subframe is a resource block (RB). There are Ω RBs per subframe. The actual data bits delivered in a RB depends on the channel quality. Let $C_{i,j}$ (bits/RB) be the channel rate of UE_i in $Cell_j$. The optimization problem asks

how to schedule the data from these M cells to N UEs by choosing proper DRX parameters for each UE_i, including DRX-cycle-length (T_i), DRX-start-offset (Z_i), On-duration (O_i) and InactivityTimer (I_i), such that more UEs can be served without violating their QoS requirements in terms of their delay constraints and admitted data rates while the total number of wake-up subframes of UEs is minimal.

Theorem 1 *The joint resource allocation and sleep scheduling problem is NP-complete.*

Proof To simplify the proof, we consider a special case where the delay constraints of UEs are identical, i.e., $D_i = D_1,\ i = 2, \ldots, N$. Hence, the best DRX-cycle-length of UE_i, i.e., T_i, should be the same as its delay constraint D_i and the best InactivityTimer I_i should be 0. In addition, we consider the case of no spatial reuse when cells serve UEs. We formulate the resource allocation problem as a decision problem, called the *DPS with DRX scheduling decision* (DDSD) problem, which is stated as follows: Given N UEs and M cells, where each $UE_i,\ i = 1, \ldots, N$ can be served cooperatively by the designated cells among $Cell_j$, $j = 1, \ldots, M$, we ask whether or not there exists a subset of UEs, denoted by S, such that the total throughput is P and the number of allocated subframes from the designated $Cell_j$ is no more than its capacity C_j. We show that the DDSD problem is NP-complete.

We first show that the DDSD problem belongs to NP. Given a problem instance and a solution containing the scheduling result, it can be verified whether or not the solution is valid in polynomial time. Thus, this part is proved. We then reduce the *multi-dimensional knapsack* (MDK) problem [17], which is known to be NP-complete, to the DDSD problem. Consider that there are N objects to be packed into an M-dimensional knapsack. Every $object_i$ has a weight $w_{i,j}$ (≥ 0) when packing the knapsack in the j-th dimension, and has a profit d_i if all its dimensional weights are packed successfully. Note that the knapsack has a capacity constraint in the j-th dimension of C_j. The MDK problem asks whether or not we can pack a subset of objects such that the total object profit is P and the total weights of the packed objects in the j-th dimension of the knapsack are no larger than C_j.

We then construct an instance of the DDSD problem as follows. Let N be the number of UEs and M be the number of cells. Each $UE_i,\ i = 1, \ldots, N$, can be served cooperatively by the designated j-th cell, $j = 1, \ldots, M$. If UE_i is served by all its designed j-th cells, it can contribute its throughput demand d_i and $Cell_j$ should allocate $w_{i,j}$ subframes to transmit its data. The total subframe capacity for each $Cell_j$ is C_j. Our goal is to determine a subset of UEs that contributes a total throughput P under the capacity constraint of each cell. We show that the MDK problem has a solution if and only if the DDSD problem has a solution.

Suppose that we have a solution to the DDSD problem such that there is a subset S of scheduled UEs and each scheduled $UE_i \in S$ needs to retrieve $w_{i,j}$ subframes from each designated $Cell_j$ to satisfy its demand. In addition, the total allocated subframes from $Cell_j$ cannot exceed its subframe space C_j and the total throughput demands of all scheduled UEs is P. By viewing the selection of UEs as the selection of objects and the subframes of the M cells as the M-dimensional knapsack, the serving results S constitute a solution to the MDK problem. This proves the *if* part.

Conversely, let an object subset $S = \{\ldots, object_i, object_{i+1}, object_{i+2}\ldots\}$ be a solution to the MDK problem. We select UE_i according to the index of the objects from such a subset that contributes throughput d_i and requires $w_{i,j}$ subframes from $Cell_j$ to transmit its demand. In this way, the total throughput of the selected UEs is P and the total number of allocated subframes in $Cell_j$ is no larger than C_j. This constitutes a solution to the DDSD problem, proving the *only if* part. □

4 Proposed schemes

Since this problem is NP-complete, finding an optimal solution is impractical. We propose two energy-efficient heuristics: SR and CA schemes, each with three stages, as illustrated in Fig. 4. Stage 1 determines DRX-cycle-length by considering each UE's delay constraint and classifies UEs with the same DRX-cycle-length into the same set. Stage 2 determines data scheduling order and DRX-start-offset. Specifically, it first chooses the cells containing the most un-served UEs. Then, SR exploits the remaining serving time ratio to pair cells with UEs; on the other hand, CA exploits two different cost metrics to make decisions. During this step, it has to guarantee that the chosen cell-UE pair is interference-free with the existing scheduling. Finally, it determines the DRX-start-offset. In Stage 3, both schemes optimize On-duration and InactivityTimer by three special rules to reduce each UE's expected wake-up ratio. The details are described as follows.

4.1 Scheduling details

Stage 1: Determining DRX-cycle-length (T_i)

To decide T_i for each UE_i, we first find the strictest delay requirement of each UE_i served in $Cell_i^{set}$, denoted as D_i^{min}, i.e.,

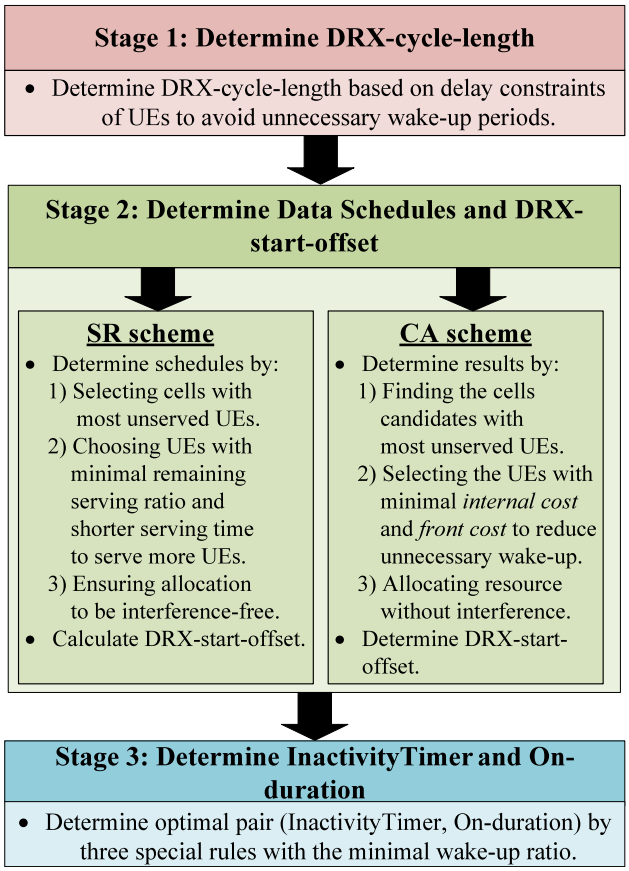

Fig. 4 Workflow of our proposed schemes

$$D_i^{min} = min_j\{D_{i,j}|Cell_j \in Cell_i^{set}\}. \quad (1)$$

Without loss of generality, let $D_1^{min} \le D_2^{min} \le \cdots \le D_N^{min}$. Then, we set $T_1 = D_1^{min}$ and set T_i, $i = 2, \ldots, N$, as follows:

$$T_i = \left\lfloor \frac{D_i^{min}}{T_{i-1}} \right\rfloor \times T_{i-1}. \quad (2)$$

Equation (1) implies $T_i \le D_i^{min}$ for each UE_i, which guarantees the receiving data to meet the delay constraint. Meanwhile, it makes T_i an integer multiple of T_{i-1}, which can help UEs to interleave their wake-up periods to avoid resource competition. Note that the allocation results will repeat after T_N/T_1 cycles.

Next, we classify UEs with the same DRX-cycle-length into the same set and sort them according to their cycle-lengths in an ascending order. Without loss of generality, we have X classes of UEs, denoted by $Class_x$, $x = 1, \ldots, X$, each with a cycle-length L_x. These classes of UEs will be scheduled sequentially in Stage 2.

Stage 2 (SR scheme): Determining Data Scheduling and DRX-start-offset (Z_i)

The main idea is to select the cells with the most un-served UEs and schedule transmissions to those UEs with the minimal required resource. In this way, subframes are better utilized, potentially reducing the wake-up intervals incurred by other UEs while increasing the number of served UEs. Let f^{cur} be the subframe index that is currently available to serve UEs; initially, $f^{cur} = 1$. Then, let $InfCell_{f^{cur}}$ be the cells that will cause interference to the current allocation results at Subframe f^{cur}; initially, $InfCell_{f^{cur}} = \phi$. Denote $Subframe_{i,j,k}^{Alloc} \in \{0, 1\}$ as the scheduling matrix, where $Cell_j$ serves UE_i at Subframe k if $Subframe_{i,j,k}^{Alloc} = 1$; otherwise, $Subframe_{i,j,k}^{Alloc} = 0$. Initially, $Subframe_{i,j,k}^{Alloc} = 0$ for all i, j, and k. We also define $Subframe_{i,j}^{Start}$ as the start subframe number of $Cell_j$ for allocating RBs to UE_i; initially, $Subframe_{i,j}^{Start} = 0$ for all i, j. Let UE_j^{UnServ} be the set of UEs that have not been served by $Cell_j$; initially, $UE_j^{UnServ} = \{UE_i|UE_i \in Class_x, Cell_j \in Cell_i^{set}\}$, for $j = 1, \ldots, M$. Then, we let S_i^{Alloc} be the number of subframes that have been allocated to UE_i. With these, we define the *remaining serving time ratio* to quantify the requirements for each UE_i with $Cell_j \in Cell_i^{set}$:

$$Ratio_i^{Remain} = \frac{(\Sigma_j S_{i,j}) - S_i^{Alloc}}{\Sigma_j S_{i,j}}, \quad (3)$$

where $S_{i,j} = \left\lceil \frac{\left\lceil \frac{R_{i,j} \times T_i}{\overline{C_{i,j}} - 3\sigma_{i,j}} \right\rceil}{\Omega} \right\rceil$ is the estimated number of sub-frames for the serving cell $Cell_j \in Cell_i^{set}$ to serve UE_i, $R_{i,j} \times T_i$ is the total number of data bits that will arrive during the cycle T_i of UE_i, and $\overline{C_{i,j}} - 3\sigma_{i,j}$ is the worst channel rate acquired from historical information. According to this ratio, we iteratively choose the un-served UE with the minimal serving ratio to be served until all UEs are examined or no subframe is available. The detailed steps are depicted as follows.

Step 1 For Subframe f^{cur}, we collect the interference-free cells with the maximal number of un-served UEs as candidates, denoted by $Cell^{cand} = \{Cell_{j^*}\}$, where

$$Cell_{j^*} = argmax_{\forall j \notin InfCell_{f^{cur}}}\{|UE_j^{UnServ}|\}. \quad (4)$$

If $Cell^{cand} \neq \phi$, go to Step 2 to find the serving UE. Otherwise, no cell can be scheduled and we check the next subframe as follows. If $f^{cur} + 1 \le L_x$, move to the next subframe by setting $f^{cur} = f^{cur} + 1$ and go back to Step 1; otherwise, no subframe is available for $Class_x$ and we move to the next class by setting $x = x + 1$. If $x \le X$, set $f^{cur} = 1$; otherwise, go to Step 5 to finish this stage.

Step 2 Choose the $UE_{i^*} \in UE_j^{UnServ}$ located in $Cell^{cand}$ with the minimal ratio $Ratio_i^{Remain}$ to serve:

$$UE_{i^*} = argmin_i\{Ratio_i^{Remain} > 0\}. \quad (5)$$

Step 3 If multiple cell-UE pairs match, we choose the one with the minimal required number of subframes:

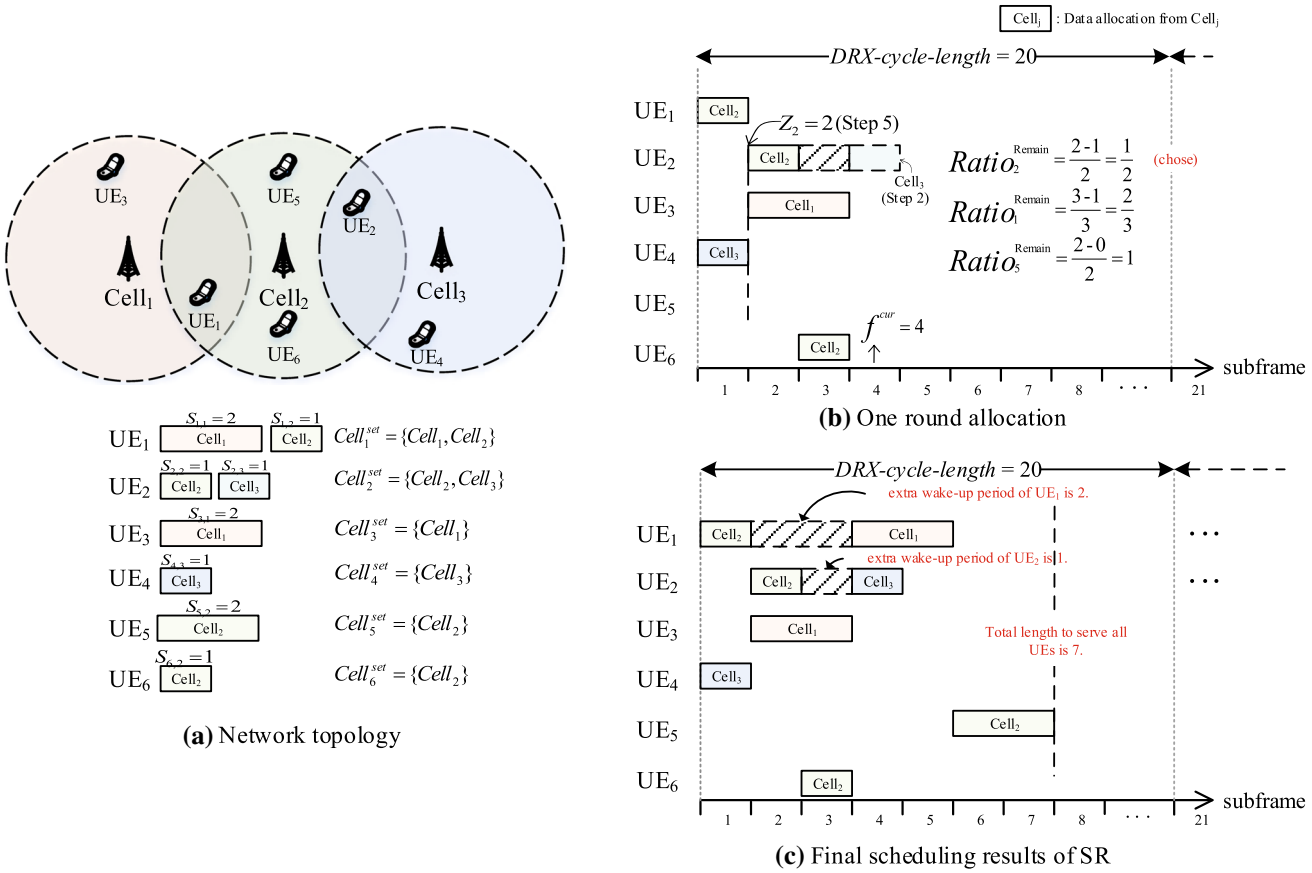

Fig. 5 Operations of stage 2 in SR

$$(Cell_{j^*}, UE_{i^*}) = argmin_j\{S_{i^*,j} | Cell_j \in (Cell_{i^*}^{set} \cap Cell^{cand})\}. \quad (6)$$

Step 4 Now, check if the the chosen pair $(Cell_{j^*}, UE_{i^*})$ can be scheduled at Subframe f^{cur} without causing interference to the existing allocation, i.e., if $Subframe_{i^*,j,f^{cur}+\Delta}^{Alloc} = 0$ for all $Cell_j \in Cell_{i^*}^{set}$ and $\Delta = 0, \ldots, S_{i^*,j^*} - 1$, we allocate S_{i^*,j^*} subframes for the pair $(Cell_{j^*}, UE_{i^*})$ at Subframe f^{cur}, and update the scheduling matrix by $Subframe_{i^*,j^*,f^{cur}+\Delta+y\cdot L_x}^{Alloc} = 1$ and the interfering cell set by $InfCell_{f^{cur}+\Delta+y\cdot L_x} = InfCell_{f^{cur}+\Delta+y\cdot L_x} \cup Cell_{i^*}^{set}$, for $\Delta = 0, \ldots, S_{i^*,j^*} - 1$, $y = 0, \ldots, (\frac{L_x}{L_x} - 1)$. Then, mark the start point of pair $(Cell_{j^*}, UE_{i^*})$ by $Subframe_{i^*,j^*}^{Start} = f^{cur}$, update the total allocated subframes by $S_{i^*}^{Alloc} = S_{i^*}^{Alloc} + S_{i^*,j^*}$, and remove UE_{i^*} from $UE_{j^*}^{UnServ}$. Otherwise, add $Cell_{j^*}$ to $InfCell_{f^{cur}}$ and go back to Step 1 to find the next candidate pair.

Step 5 Based on the above results, we set the DRX-start-offset Z_i for each UE_i, $i = 1, \ldots, N$, by

$$Z_i = min\{Subframe_{i,j}^{Start} | Cell_j \in Cell_i^{set}\}. \quad (7)$$

Below, we give an example in Fig. 5 to show one round operation of Stage 2 in SR. We consider the network in Fig. 5(a) with $Cell_1 \sim Cell_3$ serving $UE_1 \sim UE_6$, where serving cells of UEs are $Cell_1^{set} = \{Cell_1, Cell_2\}$, $Cell_2^{set} = \{Cell_2, Cell_3\}$, $Cell_3^{set} = \{Cell_1\}$, $Cell_4^{set} = \{Cell_3\}$, $Cell_5^{set} = \{Cell_2\}$, and $Cell_6^{set} = \{Cell_2\}$. Let the serving times of UEs be $S_{1,1} = 2$, $S_{1,2} = 1$, $S_{2,2} = 1$, $S_{2,3} = 1$, $S_{3,1} = 2$, $S_{4,3} = 1$, $S_{5,2} = 2$, and $S_{6,2} = 1$. Here, we assume that the schedules have been operated for 5 rounds and several pairs have been scheduled, including ($Cell_2$,UE_1) and ($Cell_3$,UE_4) at Subframe 1, ($Cell_2$,UE_2) and ($Cell_1$,UE_3) at Subframe 2, and ($Cell_2$,UE_6) at Subframe 3 (cycle length = 20 subframes). Now, we consider the current available subframe index $f^{cur} = 4$. Initially, $InfCell_4 = \phi$. In Fig. 5(b), Step 1 selects $Cell_1$, $Cell_2$, and $Cell_3$ as the candidate cells because they are interference-free and have the maximal number of un-served UEs, i.e., $|UE_1^{UnServ}| = |\{UE_1\}| = 1$, $|UE_2^{UnServ}| = |\{UE_5\}| = 1$, $|UE_3^{UnServ}| = |\{UE_2\}| = 1$. In Step 2, from the candidate set $\{Cell_1, Cell_2, Cell_3\}$, UE_2 is selected because its remaining serving ratio is the minimal, i.e., $Ratio_2^{Remain} = \frac{1}{2} < Ratio_1^{Remain} = \frac{2}{3} < Ratio_5^{Remain} = 1$. In Step 3, since ($Cell_3$, UE_2) is the only candidate pair, Step 4 then allocates its service time $S_{2,3}$ at Subframe $f^{cur} = 4$, updates the scheduling matrix by $Subframe_{2,3,4}^{Alloc} = Subframe_{2,3,4+20}^{Alloc} = \cdots = 1$, and selects the interference

cell as $InfCell_4 = InfCell_{4+20} = \cdots = \phi \cup \{Cell_2, Cell_3\}$. The starting point of the allocation is marked by $Subframe_{2,3}^{Start} = 4$ and the current allocation result is also updated by $S_2^{Alloc} = 1 + 1 = 2$ accordingly. Finally, Step 5 sets DRX-start-offset by $Z_2 = \min\{Subframe_{2,j}^{Start} | j = 2, 3\} = \min\{2, 4\} = 2$, which is the subframe index of the first allocation for UE_2. The final scheduling results are shown in Fig. 5(c).

Stage 2 (CA scheme): Determining Data Scheduling and DRX-start-offset (Z_i)

Steps 1, 4, 5 of CA are the same as those of SR. Steps 2 and 3 of CA leverage two metric functions to select cell-UE pairs. The details are described as follows.

Step 2 We define a metric function, called *internal cost* $IC_{i,j}$, to evaluate the number of extra wake-up subframes that will be incurred when we schedule $S_{i,j}$, i.e.,

$$IC_{i,j} = |UE^{Sch}| \times S_{i,j}, \tag{8}$$

where $UE^{Sch} = \{UE_{i'} | i' \in (UE_j^{UnServ} - UE_i), S_{i'}^{Alloc} > 0\}$ is the set of UEs that have been scheduled parts of their serving time. Then, we find the cell-UE pairs with the minimal $IC_{i,j}$ as follows:

$$\begin{aligned}&(Cell_{j^*}, UE_{i^*}) \\ &\quad = argmin_{i,j}\{IC_{i,j} | UE_i \text{ in } Cell_j, Cell_j \in Cell^{Cand}\}.\end{aligned} \tag{9}$$

Here, if there are multiple candidate pairs, we choose the UE with the minimal $Ratio_i^{Remain}$ to serve first. However, if there are still multiple pairs, go to Step 3; otherwise, go to Steps 4 and 5 to allocate the schedule and update the DRX parameters.

Step 3 We define another metric function, called *front cost* $FC_{i,j}$, to evaluate the extra subframes that will be incurred in front of the scheduling results of un-served UEs when scheduling $S_{i,j}$, i.e.,

$$FC_{i,j} = \sum_{j' \in Cell_i^{set}} |UE_{j'}^{UnServ}| \times S_{i,j}. \tag{10}$$

Then, we find the cell-UE pairs with the minimal $FC_{i,j}$ as follows:

$$\begin{aligned}&(Cell_{j^*}, UE_{i^*}) \\ &\quad = argmin_{i,j}\{FC_{i,j} | (Cell_j, UE_i) \text{ from (9) }\}.\end{aligned} \tag{11}$$

In the following, we show an example in Fig. 6 running two rounds of CA. We consider the same network topology as in Fig. 5(a). Now, the current subframe index is $f^{cur} = 1$. In Fig. 6(a), Step 1 selects $Cell_2$ as the candidate cell because it has the maximal number of un-served UEs, i.e., $|UE_2^{UnServ}| = |\{UE_1, UE_2, UE_5, UE_6\}| = 4$. In Step 2, since there are multiple cell-UE pairs with the same internal cost (i.e., $IC_{i,2} = 0$, for $i = 1, 2, 5, 6$) and remaining service ratio (i.e., $Ratio_i^{Remain} = 1$, for $i = 1, 2, 5, 6$), it then goes to Step 3 to calculate the front cost for those pairs and chooses the one with the minimal cost in order to reduce the extra subframes in front of the schedules. This can potentially increase the spectrum utilization. We use Fig. 6(a)i–ii to show different cell-UE pairs incurring different front costs. Since the pair $(Cell_2, UE_6)$ has the minimal cost, i.e., $FC_{6,2} = |UE_2^{UnServ}| \times S_{6,2} = |\{UE_1, UE_2, UE_5\}| \times 1 = 3 \times 1 = 3$, $Cell_2$ is selected to serve UE_6 and service time $S_{6,2}$ is allocated at Subframe $f^{cur} = 1$. Finally, the corresponding parameters are updated accordingly. The above steps are operated similarly to schedule the following pairs: $(Cell_3, UE_4)$ and $(Cell_1, UE_3)$ at Subframe 1, and $(Cell_2, UE_2)$ at Subframe 2. Now, we consider Subframe $f^{cur} = 3$. Figure 6(b) shows that Step 1 selects $Cell_2$ as the candidate cell similarly because it has the maximal number of un-served UEs, i.e., $|UE_2^{UnServ}| = |\{UE_1, UE_5\}| = 2$. In Step 2, the internal cost is calculated for each candidate pair, i.e., $IC_{i,2}, i = 1, 5$. The one with the minimal cost is identified. Figure 6(b)i–ii show how to calculate internal costs for different cell-UE pairs. Since the pair $(Cell_2, UE_1)$ has the minimal cost, i.e., $IC_{1,2} = |UE^{Sch}| \times S_{1,2} = |\{UE_2\}| \times 1 = 1 \times 1 = 1$, $Cell_2$ is chosen to serve UE_1 and allocates service time $S_{1,2}$ is scheduled at Subframe $f^{cur} = 3$. Finally, the parameters are updated accordingly. The final scheduling results are shown in Fig. 6(c).

To summarize, by both SR and CA schemes, Stage 2 can determine the allocation of serving cell-UE pairs and DRX-start-offset Z_i for each UE_i, $i = 1, \ldots, N$.

Stage 3: Optimizing DRX parameters (I_i and O_i)

The goal of this stage is to determine the best InactivityTimer I_i and On-duration O_i for each UE_i to reduce unnecessary wake-up periods. Recall that $Subframe_{i,j}^{Start}$ is the start subframe determined in Stage 2. Below, we calculate the wake-up ratio for each UE_i, I_i, and O_i based on [26]. Specifically, we first define ER_i^{WakeUp} to represent the expected wake-up ratio of UE_i:

$$ER_i^{WakeUp} = \frac{max\{(EPO_i^{max} - Z_i), O_i\} + I_i}{T_i}, \tag{12}$$

where

$$EPO_i^{max} = max\{EPO_{i,j} | Cell_j \in Cell_i^{set}\} \tag{13}$$

is the maximal expected end subframe number for the pair $(Cell_j, UE_i)$, and

$$EPO_{i,j} = Subframe_{i,j}^{Start} + \left\lceil \frac{\lceil \frac{R_{i,j} \times T_i}{E(C_{i,j})} \rceil}{\Omega} \right\rceil \tag{14}$$

is the expected end subframe for the pair $(Cell_j, UE_i)$ and $\left\lceil \frac{\lceil \frac{R_{i,j} \times T_i}{E(C_{i,j})} \rceil}{\Omega} \right\rceil$ is the expected data reception time (in subframes)

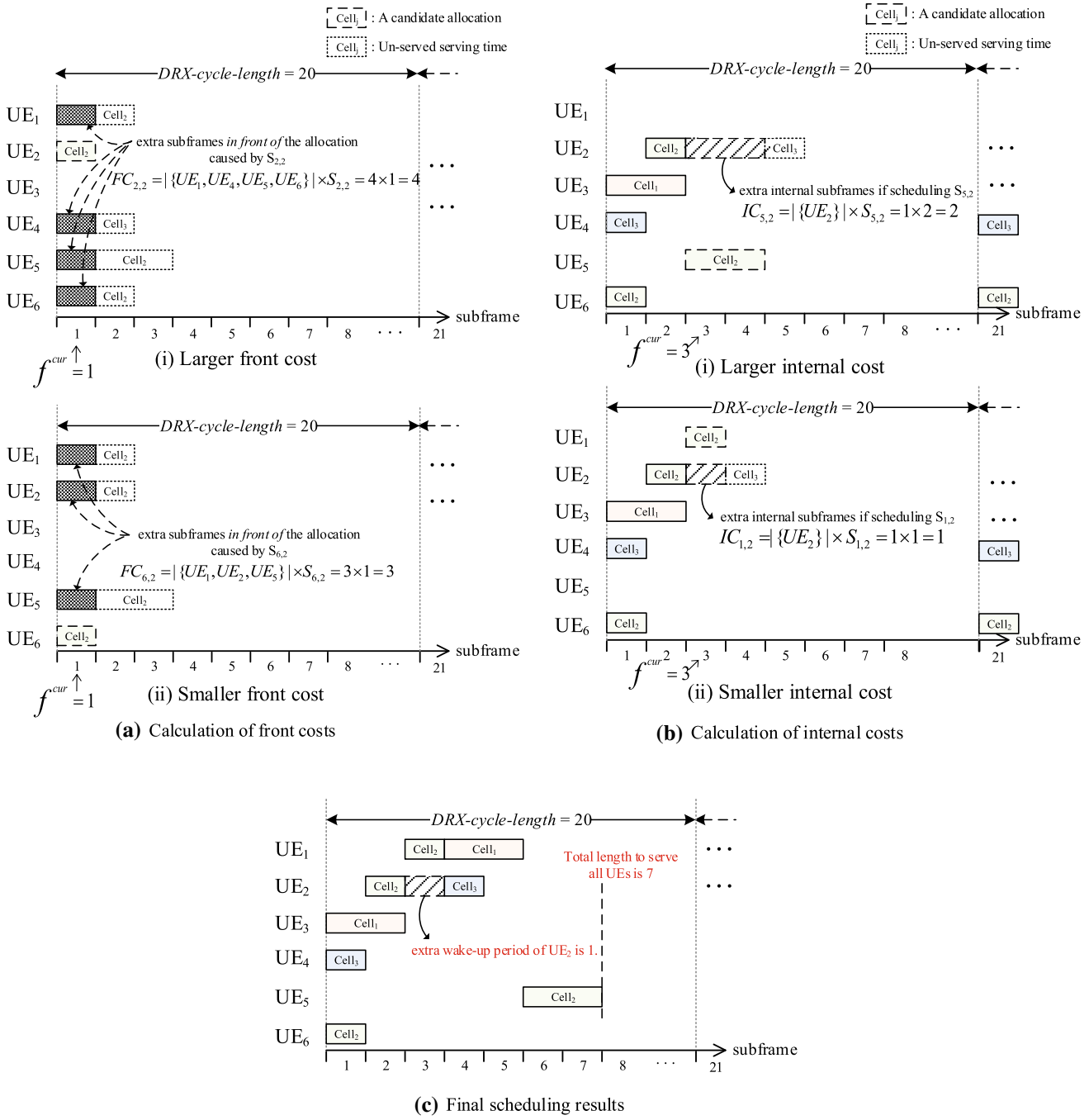

Fig. 6 Operations of stage 2 in CA

for UE_i from $Cell_j$. Note that $E(C_{i,j})$ is the expected channel rate for $Cell_j$ serving UE_i.

Second, we design three rules to find feasible (I_i, O_i) pairs. Then, we choose the pair with the minimal expected number of wake-up subframes.

- *Rule 1* Set $I_i = 0$ and $O_i = max\{Subframe_{i,j}^{Start} + S_{i,j} | Cell_j \in Cell_i^{set}\} - Z_i$.
- *Rule 2* Set $I_i = 1$ and $O_i = (max\{Subframe_{i,j}^{Start} | Cell_j \in Cell_i^{set}\} - Z_i) + 1$.
- *Rule 3* Set $I_i = max\{h_{i,k}\} + 1$ and $O_i = min\{Subframe_{i,j}^{Start} + S_{i,j} | Cell_j \in Cell_i^{set}\} - Z_i$, where $h_{i,k}$ is the k-th idle period of UE_i.

Note that Rule 1 favors shorter InactivityTimer and longer On-duration, Rule 2 favors longer InactivityTimer and

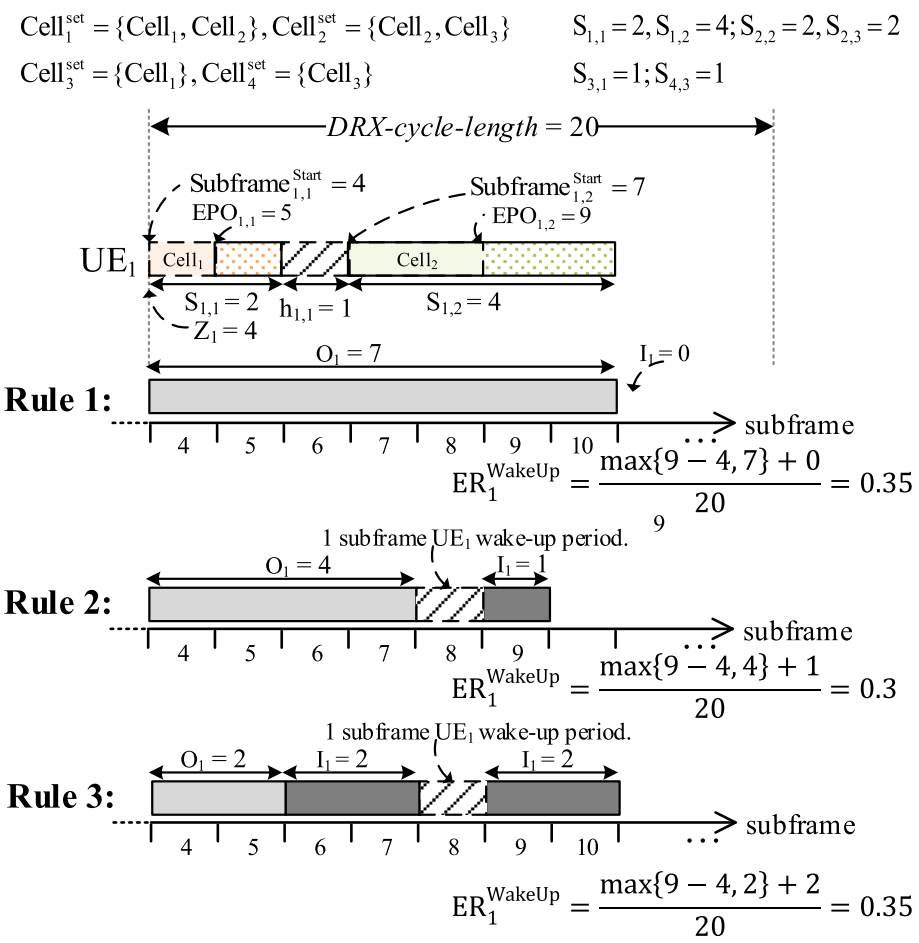

Fig. 7 An example of determining the best pair of on-duration and InactivityTimer

shorter On-duration, and Rule 3 ensures UEs to get all data from separated wake-up periods. Based on these rules, we can evaluate the expected wake-up ratio and choose the pair with the minimal expected wake-up ratio. An example of the effect of different rules is shown in Fig. 7. In this example, the service times of UE_1 are $S_{1,1} = 2$ and $S_{1,2} = 4$, which are scheduled at Subframes 4–5 and 7–10, respectively. Thus, the start subframes are $Subframe_{1,1}^{Start} = 4$ and $Subframe_{1,2}^{Start} = 7$. Assume that there is an idle period $h_{1,1} = 1$ between the two service times. Based on the three rules, the best pair is $O_1 = 4$ and $I_1 = 1$ due to $min\{0.35, 0.3, 0.35\} = 0.3$. Finally, we choose the pair that incurs the minimal expected wake-up ratio for each UE_i.

4.2 Computational complexity analysis

For SR, Stage 1 costs $O(NlogN)$ operations to sort UEs and determine their cycle lengths T_i. For Stage 2, Step 1 costs $O(MlogM)$ operations to sort cells and $O(1)$ operations to choose cells containing the most un-served UEs. In Step 2, it costs $O(N)$ operations to choose UEs with the minimal remaining serving ratio and further choose UEs with the minimal serving time. In Step 3, it costs $O(N + M)$ operations to pair a UE with a cell. Since this scheme executes Step 1 for $O(T_N)$ iterations at most and Steps 2–4 for $O(M)$ iterations, respectively, the complexity of Stage 2 is $O(T_N) \cdot (O(MlogM) + O(M) \cdot O(N + M)) = O(T_N M(N + M))$. For Stage 3, it costs $O(N)$ operations to determine the best On-duration and InactivityTimer pair. Therefore, SR costs a total of $O(NlogN) + O(T_N M(N + M)) + O(N) = O(NlogN + T_N M(N + M))$ operations.

For CA, Stage 1 and Stage 3 are the same as SR, so they cost $O(NlogN)$ and $O(N)$ operations, respectively. For Stage 2, Step 1 is the same as SR, costing $O(MlogM) + O(1)$ operations. In Step 2, it costs $O(N^2)$ operations to choose the UE with the minimal internal cost because each UE must consider internal costs of all other UEs. In Step 3, it costs $O(N)$ operations to choose the UE with the minimal front cost. Since this scheme also executes Step 1 for

$O(T_N)$ iterations and Steps 2–4 for $O(M)$ iterations, the complexity of Stage 2 is $O(T_N) \cdot (O(MlogM) + O(M) \cdot O(N^2)) = O(T_N M(logM + N^2))$. Therefore, CA costs a total of $O(NlogN) + O(T_N M(logM + N^2)) + O(N) = O(T_N M(logM + N^2))$ operations.

Note that since T_N is a constant, the complexities of SR and CA are $O(NlogN)$ and $O(N^2)$ if $N >> M$, respectively.

5 Simulation results

We developed a C++ simulator to verify the effectiveness of our scheme.[2] The system parameters [28] are listed as follows. The frame duration is 10 ms. The channel bandwidth is 20 MHz; thus, we have $\Omega = 100$ RBs in each subframe. The cell radius is 500 m. The BS Tx power is 23 dBm. The thermal noise is −174 dBm/Hz. The antenna gains of UEs and cells are 0 dBi and 14 dBi, respectively. The traffic models are summarized in Table 1. The numbers of cells and UEs are $M = 25$ and $N = 300 \sim 3000$, respectively. The cells are deployed in hexagons and the cell distance between neighboring cell centers is 0.866 km [29]. UEs are distributed uniformly and apply a random walk with a speed of 1.4 m/s [30].

We compare our schemes against the throughput-aware cell-selection (TA-CS) [9], instantaneous-load DPS (IL-DPS), proportional-fairness DPS (PF-DPS) [11], and multi-cell selection scheme (MCS) [7] schemes. TA-CS applies a throughput-aware profit function to pair UEs with cells in order to efficiently utilize network resource. IL-DPS and PF-DPS use a number of active UEs and proportional fairness metrics as the cell-selection method. MCS uses the link rates of cells and the number of active UEs to pair UEs. Since TA-CS does not design subframe-level scheduling, we apply round-robin scheduling (same as MCS) in our simulations.

We consider six performance metrics: (1) *number of served UEs*: the total number of UEs that can be served while ensuring their QoS requirements; (2) *system throughput*: the total number of data bits received by the UEs per cell during the experiment period; (3) *satisfaction ratio*: the average serving ratio of all UEs; i.e., $ratio = \frac{\sum_i S_i^{Alloc}}{\sum_i \sum_j S_{i,j}}$; (4) *resource utilization*: the allocated resource over the total available resource; (5) *average wake-up ratio*: the ratio of wake-up subframes over the total execution subframes; (6) *total energy consumption*: the total consumed energy for all UEs, where the power model is referred to [33]. Note that each simulation result is averaged by at least 1000 experiments.

[2] As far as we know, ns-3 [27] does not support the C-RAN model in terms of channel estimation and access procedure.

Table 1 Traffic models [31, 32]

Service type	Bit rate (Kbps)	Packet delay constraint (ms)
VoIP	64	100
IPTV	128	300
HTTP/FTP	256	300

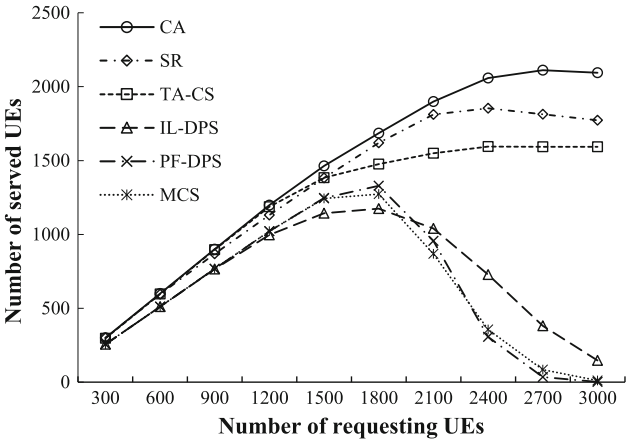

Fig. 8 Comparisons on the number of served UEs

5.1 Number of served UEs

First, we investigate the effects of the number of requesting UEs on the number of served UEs. As shown in Fig. 8, IL-DPS, PF-DPS, and MCS serve the fewest UEs because each UE is paired with a single cell without considering cooperative transmission [this can be validated by Fig. 10(a)]. TA-CS exploits DPS and estimates the throughput between cells and UEs; thus, it can serve more UEs, especially the edge UEs [referring to Fig. 10(b)]. However, when the number of UEs is larger than 2400, TA-CS prefers to serve the center UEs, which limits its performance [referring to Fig. 10(a) and (b)]. Our two schemes perform the best because they consider the cells with the most un-served UEs when scheduling. Besides, CA outperforms SR because it additionally considers both internal cost and front cost when serving UE, thus scheduling resources more efficiently (this will be clear later in Fig. 12). In average, SR and CA can serve 13% and 23% more UEs, respectively, compared to TA-CS.

5.2 System throughput

Second, we investigate the effects of the number of requesting UEs on system throughput. As shown in Fig. 9,

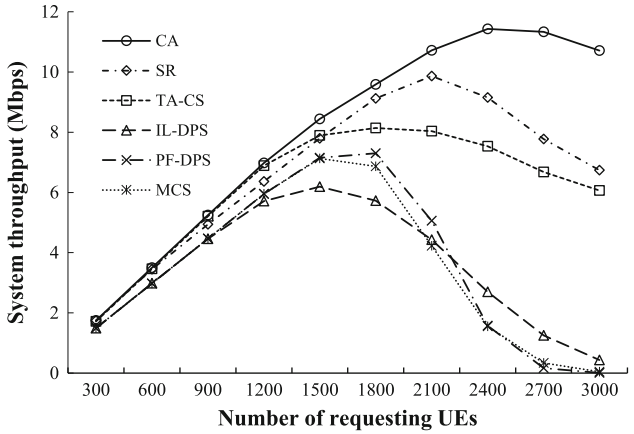

Fig. 9 Comparisons on system throughput

IL-DPS, PF-DPS, and MCS all have low throughputs because they pair all UEs with cells individually without considering cooperative transmission [referring to Fig. 10(a)]. TA-CS has a higher throughput than the above schemes because it cooperates multiple cells to serve the edge UEs [referring to Fig. 10(b)]. SR considers the remaining serving ratio when it determines the allocation order; thus, more data can be transmitted completely. Besides, CA outperforms all other schemes because it determines the allocation order based on two special cost metrics to better utilize resource (this can be seen later in Fig. 12). In average, SR and CA can increase 17% and 25% of system throughput, respectively, compared to TA-CS.

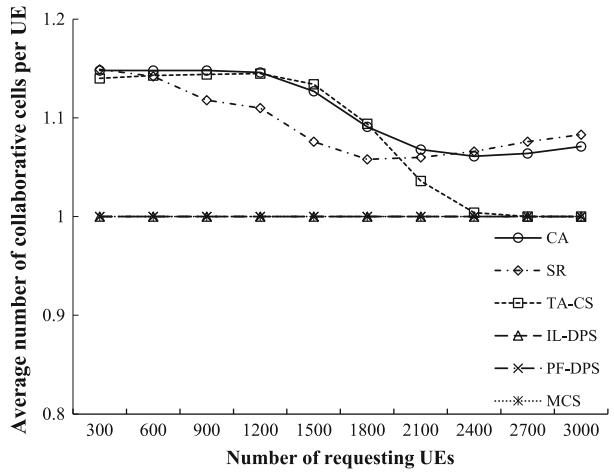

(a) Comparisons on the average number of collaborative cells per UE.

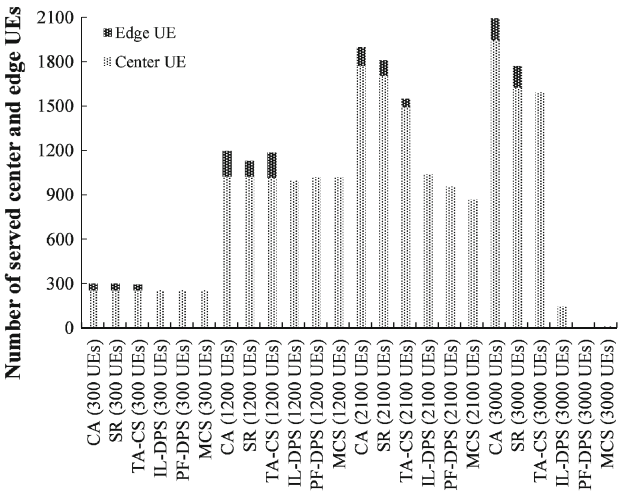

(b) Comparisons on served center and edge UEs.

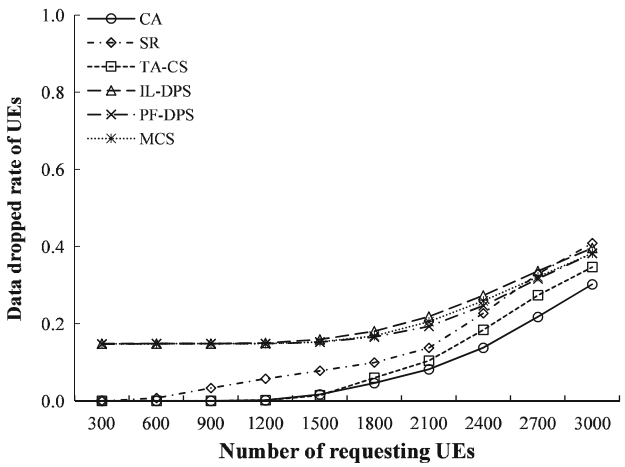

(c) Comparisons on data dropped rate of UEs.

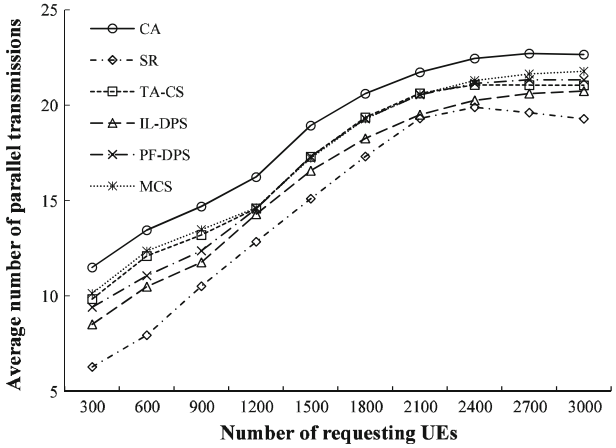

(d) Comparisons on average number of parallel transmissions.

Fig. 10 Extensive results to support our explanation

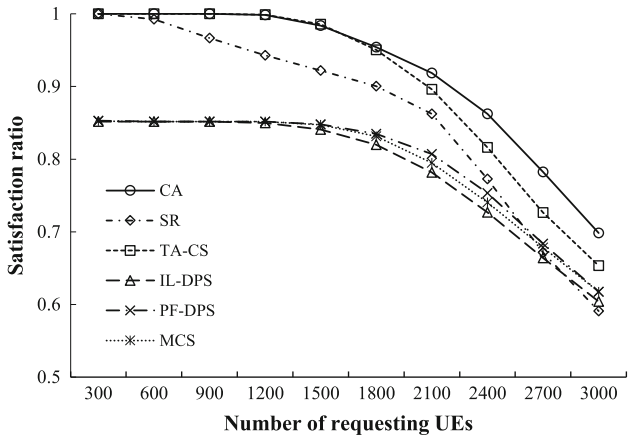

Fig. 11 Comparisons on satisfaction ratio

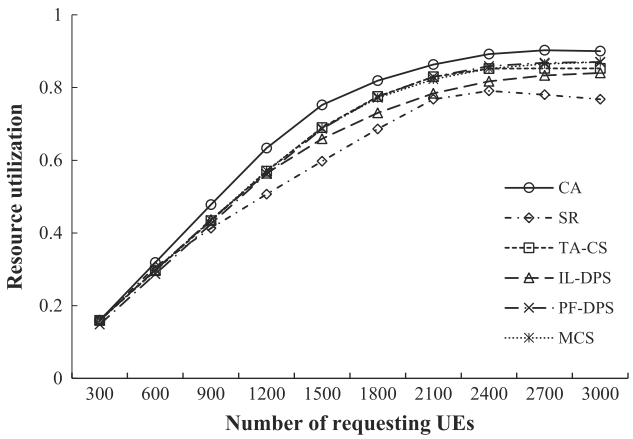

Fig. 12 Comparisons on resource utilization

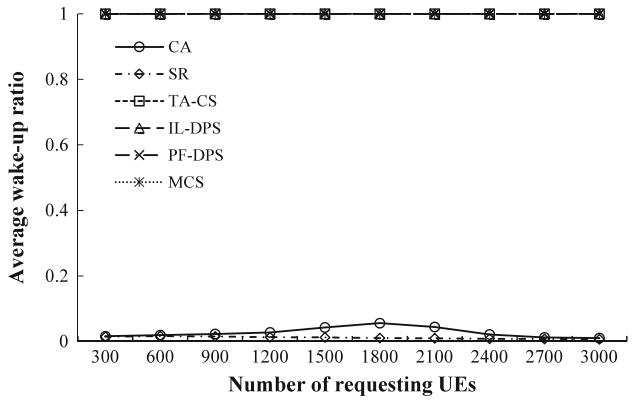

Fig. 13 Comparisons on average wake-up ratio

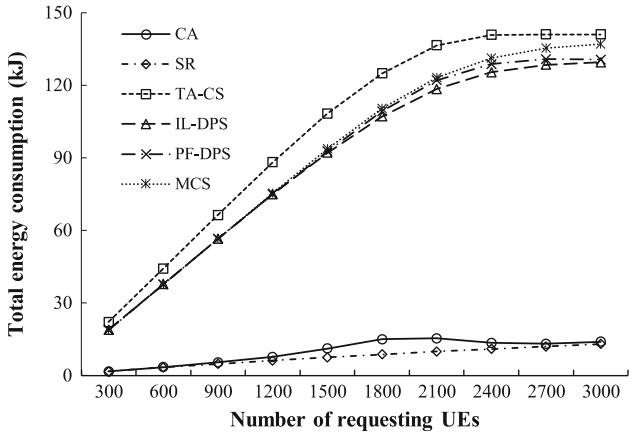

Fig. 14 Comparisons on total energy consumption

5.3 Satisfaction ratio

Next, we investigate the effects of the number of requesting UEs on the satisfaction ratio. As shown in Fig. 11, the satisfaction ratio decreases as the number of requesting UEs increases. IL-DPS, PF-DPS, and MCS have lower satisfaction ratio because they neglect the subframe-level scheduling and collaborative transmission [referring to Fig. 10(a) and (b)]; thus, most of data are dropped due to delay violation [referring to Fig. 10(c)]. Since SR applies the remaining serving ratio to serve UEs, more unsatisfied UEs can be served in advance. TA-CS is better than SR because it can estimate the instantaneous throughput between cells and UEs. CA outperforms all others because it applies the front cost metric to fully utilize resources (this will be shown later in Fig. 12). CA can increase up to 7% of satisfaction ratio, compared to TA-CS.

5.4 Resource utilization

Next, we investigate the effects of the number of requesting UEs on resource utilization. As shown in Fig. 12, the resource utilization increases as the number of requesting UEs increases. SR has the lowest resource utilization because it always chooses the UEs with shorter serving time and may harm spatial reuse [this can be evidenced by Fig. 10(d)]. IL-DPS, PF-DPS, MCS, and TA-CS perform better because they allocate resources sequentially when it is interference-free; thus, they can utilize resource due to higher spatial reuse efficiency. CA has the best resource utilization because of its better scheduling strategies. CA can increase up to 9% of resource utilization, compared to TA-CS.

5.5 Average wake-up ratio

Figure 13 investigates the effects of the number of requesting UEs on average wake-up ratio. TA-CS, IL-DPS,

PF-DPS, and MCS neglect to optimize the DRX mechanism, so we mark them as 100%. SR has a lower wake-up ratio than CA because it can serve the UEs continuously without extra wake-up time based on the serving ratio; contrarily, CA exploits both the internal cost and front cost metrics to increase resource utilization, slightly harming wake-up ratio.

5.6 Total energy consumption

Figure 14 studies the effects of the number of requesting UEs on energy consumption. TA-CS, IL-DPS, PF-DPS, and MCS all neglect the optimization of DRX mechanism, so they all have high energy cost. SR has lower energy consumption than CA because it serves UEs with remaining demand first to avoid unnecessary wake-up periods. Contrarily, CA leverages both the internal cost and front cost metrics to balance resource and energy efficiency. Note that SR and CA can reduce at least 50% of energy consumption, compared to other schemes.

6 Conclusions

This paper addresses the DRX optimization problem by considering the QoS requirements of UEs in a DPS C-RAN. We formally define the problem and prove it to be NP-complete. Two heuristics called SR and CA are then proposed. Our heuristics make insightful observations on the key factors that may impact a DRX-DPS joint scheduling, namely serving ratio, internal cost, and front cost. Their time complexities are analyzed by $O(N \log N)$ and $O(N^2)$, which are polynomial time and effective in a large-scale network. Based on these considerations, we show that the proposed schemes can outperform existing schemes significantly in terms of system throughput (17–25%), number of served UEs (13–23%), and energy consumption (at least 50%). In summary, this is the first complete work that addresses the DRX scheduling problem in a C-RAN under the DPS mode. Integrating DRX with the C-RAN framework is a challenge because in the past a UE is always served by one BS at a time. With C-RAN, DRX involves scheduling and interactions with multiple BSs. The work may lead to further studies that involve multi-BS scheduling.

Acknowledgements This research is co-sponsored by MOST 108-2218-E-006-044, 108-2813-C-182-002-E, 107-2221-E-009-173-MY3, 107-2221-E-024-001-MY3, 106-2221-E-182-015-MY3, 105-2221-E-182-051, 105-2218-E-009-003, Pervasive Artificial Intelligence Research (PAIR) Labs, "Center for Open Intelligent Connectivity" (MoE), Delta Electronics, ITRI, Institute for Information Industry, Academia Sinica, and Chang Gung Memorial Hospital, Taoyuan. Jia-Ming Liang is the corresponding author.

References

1. Sabella, D., et al. (2013). RAN as a service: Challenges of designing a flexible RAN architecture in a cloud-based heterogeneous mobile network. In *Future network and mobile summit* (pp. 1–8).
2. Solimana, S. S., & Songb, B. (2017). Fifth generation (5G) cellular and the network for tomorrow: Cognitive and cooperative approach for energy savings. *Journal of Network and Computer Applications*, *85*(1), 84–93.
3. Gupta, R., Kalyanasundaram, S., Natarajan, B., & Sen, M. (2016). Performance analysis of enhanced dynamic point selection CoMP scheme for heterogeneous networks. In *IEEE vehicular technology conference (VTC)* (pp. 1–5).
4. Michail, K., et al. (2016). A load and channel aware dynamic point selection algorithm for LTE-A CoMP networks. In *IEEE international conference on telecommunications and multimedia (TEMU)* (pp. 1–5).
5. Lee, S. H., & Sohn, I. (2015). Message-passing-based dynamic point selection for coordinated multipoint transmission. *IEEE Communications Letters*, *19*(10), 1850–1853.
6. Fernandez-Lopez, V., Soret, B., Pedersen, K. I., Steiner, J., & Mogensen, P. (2016). Sensitivity analysis of centralized dynamic cell selection. In *IEEE vehicular technology conference (VTC)* (pp. 1–5).
7. Shaverdian, A., & Rosenberg, C. (2017). On the benefits and implementation costs of multi-cell selection in heterogeneous networks. In *IEEE wireless communications and networking conference (WCNC)* (pp. 1–6).
8. De Domenico, A., Diez, L., Aguero, R., Ktenas, D., & Savin, V. (2015). EMF-aware cell selection in heterogeneous cellular networks. *IEEE Communications Letters*, *19*(2), 271–274.
9. Amzallag, D., Bar-Yehuda, R., Raz, D., & Scalosub, G. (2013). Cell selection in 4G cellular networks. *IEEE Transactions on Mobile Computing*, *12*(7), 1443–1455.
10. Karavolo, M., et al. (2017). A dynamic hybrid clustering scheme for LTE–A networks employing CoMP-DPS. In *IEEE international workshop on computer aided modeling and design of communication links and networks (CAMAD)* (pp. 1–5).
11. Agrawal, R., et al. (2014). Dynamic point selection for LTE-advanced: Algorithms and performance. In *IEEE wireless communications and networking conference (WCNC)* (pp. 1392–1397).
12. Alorainy, A., & Hossain, M. J. (2017). Cross-layer performance of downlink dynamic cell selection with random packet scheduling and partial CQI feedback in wireless networks with cell sleeping. *IEEE Transactions on Wireless Communications*, *16*(8), 5353–5369.
13. Eguizabal, M., & Hernandez, A. (2016). Joint dynamic resource allocation and load balancing-cell selection in LTE-A HetNet scenarios based on Type 1 inband relay deployments. *Computer Networks*, *100*, 90–109.
14. Liu, L., Zhou, Y., Yuan, J., Tian, L., & Shi, J. (2018). Fronthaul capacity requirement minimization via physical layer caching in cloud-RAN. In *IEEE global communications conference (GLOBECOM)* (pp. 1–6).
15. Astely, D., et al. (2009). LTE: The evolution of mobile broadband. *IEEE Communications Magazine*, *47*(4), 44–51.
16. Hsu, C.-K., Liang, J.-M., Wu, K.-R., Chen, J.-J., & Tseng, Y.-C. (2017). Energy-efficient dynamic point selection for cloud radio access networks (C-RAN). In *IEEE wireless communications and networking conference (WCNC)* (pp. 1–6).
17. Freville, A., & Plateau, G. (1994). An efficient preprocessing procedure for the multidimensional 0–1 knapsack problem. *Discrete Applied Mathematics*, *49*(1–3), 189–212.

18. Alonso, R. M., et al. (2018). TV white space and LTE network optimization toward energy efficiency in suburban and rural scenarios. *IEEE Transactions on Broadcasting*, *64*, 164–171.
19. Vincenzi, M., et al. (2017). Cooperation incentives for multi-operator C-RAN energy efficient sharing. In *IEEE international conference on communications (ICC)* (pp. 1–6).
20. Yoon, C., & Cho, D. H. (2015). Energy efficient beamforming and power allocation in dynamic TDD based C-RAN system. *IEEE Communications Letters*, *19*(10), 1806–1809.
21. Luo, S., Zhang, R., & Lim, T. J. (2015). Downlink and uplink energy minimization through user association and beamforming in C-RAN. *IEEE Transactions on Wireless Communications*, *14*(1), 494–508.
22. Tang, J., Tay, W. P., & Quek, T. Q. S. (2015). Cross-layer resource allocation with elastic service scaling in cloud radio access network. *IEEE Transactions on Wireless Communications*, *14*(9), 5068–5081.
23. Nguyen, D. H. N., Le, L. B., & Le-Ngoc, T. (2017). Optimal dynamic point selection for power minimization in multiuser downlink CoMP. *IEEE Transactions on Wireless Communications*, *16*(1), 619–633.
24. Zhao, W., & Wang, S. (2016). Traffic density-based RRH selection for power saving in C-RAN. *IEEE Journal on Selected Areas in Communications*, *34*(12), 3157–3167.
25. Arouk, O., Ksentini, A., & Taleb, T. (2016). Group paging-based energy saving for massive MTC accesses in LTE and beyond networks. *IEEE Journal on Selected Areas in Communications*, *34*(5), 1086–1102.
26. Liang, J.-M., Chen, J.-J., Hsieh, P.-C., & Tseng, Y.-C. (2016). Two-phase multicast DRX scheduling for 3GPP LTE-advanced networks. *IEEE Transaction on Mobile Computing*, *15*(7), 1839–1849.
27. NS-3 Consortium. (2018). *ns-3 network simulator*. Retrieved July 1, 2018 from https://www.nsnam.org/.
28. Hsu, P.-M., Chen, J.-J., & Liang, J.-M. (2013). Dynamic cooperating set planning for coordinated multi-point (CoMP) in LTE/LTE-advanced systems. In *IEEE Asia-Pacific network operations and management symposium (APNOMS)* (pp. 1–6).
29. Hashmi, U. S., Zaidi, S. A. R., Darbandi, A., & Imran, A. (2018). On the efficiency tradeoffs in user-centric cloud RAN. In *IEEE international conference on communications (ICC)* (pp. 1–7).
30. Deng, T., Wang, X., Fan, P., & Li, K. (2016). Modeling and performance analysis of tracking area list-based location management scheme in LTE networks. *IEEE Transactions on Vehicular Technology*, *65*(8), 6417–6431.
31. Liang, J.-M., Chen, J.-J., Cheng, H.-H., & Tseng, Y.-C. (2013). An energy-efficient sleep scheduling with QoS consideration in 3GPP LTE-advanced networks for internet of things. *IEEE Journal on Emerging and Selected Topics in Circuits and Systems*, *3*(1), 13–22.
32. Pongthaipat, N. (2008). *Demand-based wireless network design by test point reduction*. Doctoral Dissertation, University of Pittsburgh.
33. Hailu, S., et al. (2015). DRX-aware power and delay optimized scheduler for bursty traffic transmission. In *IEEE vehicular technology conference (VTC)* (pp. 1–5).
34. Camps-Mur, D., et al. (2019). 5G-XHaul: A novel wireless-optical SDN transport network to support joint 5G backhaul and fronthaul services. *IEEE Communications Magazine*, *57*, 99–105.